JOURNAL OF MATERIALS SCIENCE 20 (1985) 237–245

Failure mechanics of uPVC cyclically pressurized water pipelines

S. H. JOSEPH*, P. S. LEEVERS
Department of Mechanical Engineering, Imperial College of Science and Technology, London, SW7 2BP, UK

An extensive investigation has been directed towards explaining fatigue failure of pressurized water pipelines under service conditions, in terms of laboratory studies of the base material (unplasticized polyvinyl chloride, uPVC). It is established that many such failures are located in the regime to which linear elastic fracture mechanics can be applied, with encouraging predictive accuracy. Only failures at very low stress levels are not reliably explained by these methods, which nevertheless provide direction for further study.

1. Introduction

The importance of cyclic loading on the failure of uPVC components has long been recognized [1]. Correctly processed uPVC is a tough material [2], with high strength and creep resistance, but in applications under varying load the possibility of fatigue crack growth (FCG) must always be considered. The work described here constituted part of a broader investigation into the failure of plastic pipes under various service loading conditions, aimed towards producing data for use in design and installation. The approach used was therefore to test as-produced pipe specimens under schematized but realistic pressure histories and relate the results to material property data from parallel FCG investigations on laboratory specimens.

This relationship remains incompletely understood despite numerous, widespread and persistent investigations of uPVC pipes and pipe materials. These have focused on such parameters as processing [3–6], notching [4, 5, 7–9], cyclic frequency [4, 5], temperature [5, 10, 11], mean pressure [10, 11], and supplementary asymmetric loadings [9]; or they have presented extensive but uninterpreted fatigue life data [12–14] under normal laboratory conditions. It is hoped that the present contribution will further this understanding, by progressing from empirical observations of many pipe fatigue failures to explore the underlying mechanisms of fatigue damage on the constituent material.

2. Experimental procedure

The subjects of our experiments were specimens of uPVC pipe, produced by four different UK manufacturers to British Standards specifications, nominal Size 2: outside diameter, D, in the range 60.2 to 60.5 mm and wall thickness, t, in the range 3.1 to 3.7 mm (Class D) or in the range 3.9 to 4.5 mm (Class E). 95% of the fatigue failure sites were at wall thicknesses within 8% of the specified mean. Sections of pipe 445 mm long were washed, identified and mounted in the hydraulic cyclic pressuring rig previously described [11], each station of which permits internal pressurization between preset peak and trough levels, with an approximately trapezoidal 1 Hz waveform. In these experiments the trough pressure was held at 0.4 MPa, and the peak set to yield the desired pressure amplitude Δp; the limits were separately and continuously monitored on a chart recorder, by electronic processing of the pressure transducer signal. For the higher Δp (1.5 MPa and over) tests, each station loaded a single specimen, but for most low-Δp tests three were pressurized in parallel, each being replaced as it failed. This yielded tensile hoop strain rise rates of 0.06 or 0.02 sec^{-1},

*Present address: Department of Mechanical Engineering, Sheffield University, Mappin Street, Sheffield, UK.

0022–2461/85 $03.00 + .12

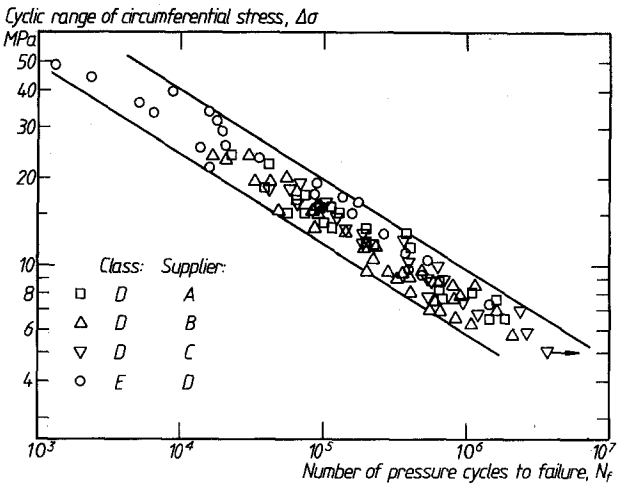

Figure 1 Circumferential stress range plotted against number of pressure cycles to failure of uPVC pipe in water at 20° C and 1 Hz.

respectively. The pressurizing medium was tap water, the environment a temperature controlled (20 ± 0.5° C) circulating filtered water bath. Special control circuits were incorporated for automatic detection of specimen leakage, or of hydraulic oil contamination of the pressurizing water, either of which terminated loading. Each failed specimen was examined externally to locate the point of leakage, always an axial crack. The surrounding material was cut out, cooled in liquid nitrogen and broken open to reveal the crack surfaces, which were examined and measured using an optical stereomicroscope and a travelling microscope. Areas of particular interest were gold-coated and examined using a Cambridge stereoscan scanning electron microscope (SEM).

3. Results and discussion

Fig. 1 shows results of over 100 pipe fatigue tests as a plot of $\log \Delta\sigma$ (circumferential stress amplitude) against $\log N$ (number of cycles to failure). The circumferential stress was calculated from internal pressure, p, as for a thin-walled tube, so that:

$$\Delta\sigma = \Delta p \frac{(D-2t)}{2t}. \qquad (1)$$

Although a single slope (i.e. exponent) of about $-1/3$ describes the whole data set, different modes of failure, varying with stress (Fig. 2) were evident even before the fracture surfaces were separated and examined.

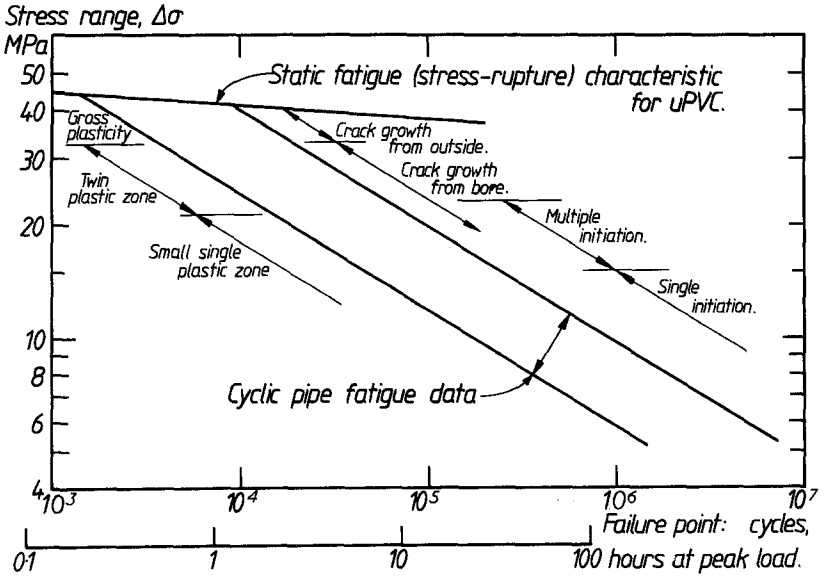

Figure 2 Static and fatigue pipe failure modes in data of Fig. 1.

3.1. Failure modes

Above a stress range of 33 MPa, pipe failure occurred within a few thousand cycles, accompanied by extensive stress-whitening and plastic deformation. The pipe swelled, necking down near the point of failure, which developed by ductile tearing from the outside surface inwards. This type of ductile rupture is commonly seen in time-to-failure tests under high static pressure, which constitute the basic method for conventional pipe lifetime prediction: the stress-rupture characteristic for a typical uPVC pressure pipe formulation [15] is mapped in Fig. 2. Clearly, at high cyclic fatigue levels, static failure intervenes before sufficient fatigue cycles can be applied for characteristic dynamic fatigue mechanisms to badly damage the pipe. The dynamic fatigue curve can confidently be extrapolated back along the static fatigue curve. This complements the previous, more general findings [10, 11] that mean pressure effects on fatigue life-time are slight until a level sufficient to bring about directly the intervention of static failure mechanisms is reached.

At stress ranges lower than 33 MPa, the cracks revealed surfaces characteristic of fatigue loading. Crack growth had progressed from an initiation point at or near the pipe bore, sometimes leaving concentric semi-elliptical bands of a distinct texture, until separation at the outer surface caused sufficient leakage to trigger termination of the test. The outside of the pipe wall then revealed a short crack surrounded by a stress-whitened zone which, for higher stresses, separated into two parallel bands (Fig. 3) representing the leading edges of twin slip lines radiating from the crack tip. At the point of breakthrough the crack itself had progressed through these (rather than, as would be expected, between them), leaving a stepped surface. This mechanism seems only to operate in the plane-stress region immediately adjacent to the surface.

At low to medium stress ranges ($15 < \Delta\sigma < 23$ MPa), an increase in $\Delta\sigma$ tended to multiply the number of crack initiation sites on the bore. For $\Delta\sigma < 15$ MPa, sectioning the plane of the leaking crack revealed no other obvious concurrent damage (Fig. 4). Stress levels above $\Delta\sigma = 15$ MPa revealed a multitude of coplanar cracks in progress (Fig. 5). Careful inspection of the bore showed these to be concentrated on three equally disposed radial planes, assumed to be weld lines from the extruder

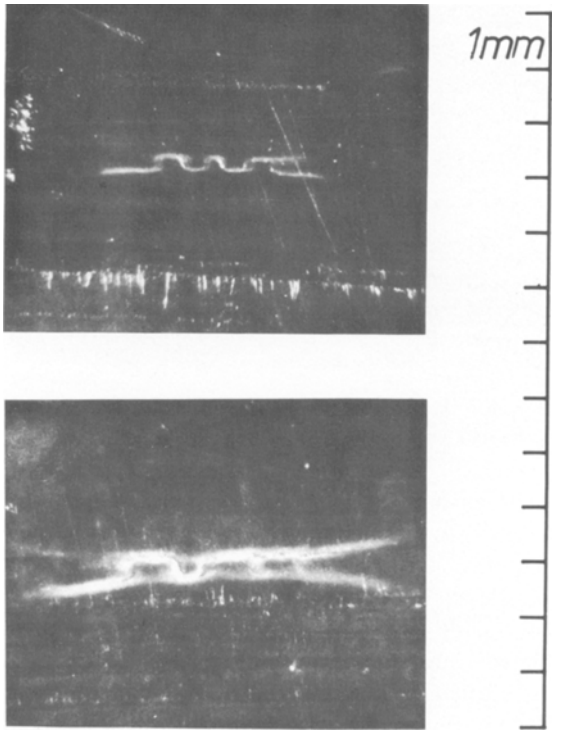

Figure 3 Appearance of crack on outside of pipe surface for intermediate (above) and high (below) stress range levels in the fatigue regime.

die spider. These observations already suggest the distance of an inherent population of flaws characteristic, to some extent, of the manufacturing process. The effect of increasing stress is to activate an increasing proportion of this population as potential origins of ultimate failure.

Fig. 4 shows a typical low-stress (10 MPa) fracture surface. At some stage on its radial expansion, the front undergoes a transition whose effect is to leave a more reflective surface texture.

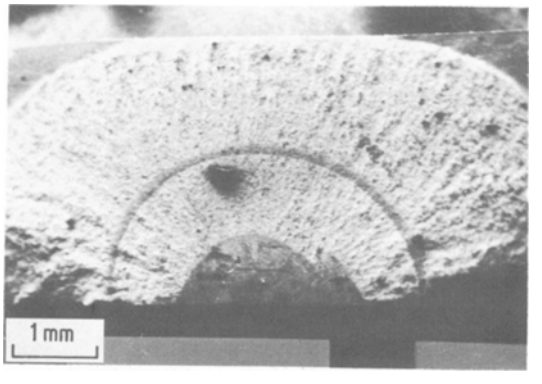

Figure 4 Typical fatigue crack surface, showing abrupt transition in surface texture.

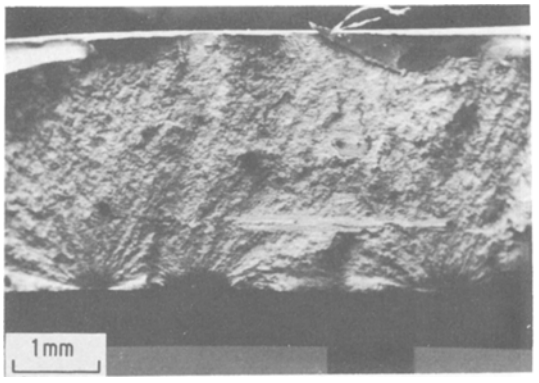

Figure 5 Multiple crack initiation sites along a pipe die spider weld line.

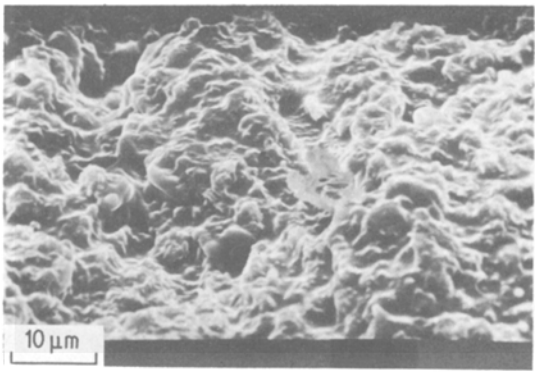

Figure 7 Detail of lighter area in Fig. 4, showing evidence of plastic flow.

SEM examination reveals the original, darker area (Fig. 6) to be smooth down to a sub-micron scale, whereas the lighter area (Fig. 7) shows traces of plastic deformation at a scale of 10 μm, typical of ductile rupture. Higher magnification (Fig. 8) shows this material to be a sponge-like mesh permeated by voids 0.1 to 1 μm in size. The abrupt change in macroscopic reflectivity is thus apparently due to a sudden change in propagation mechanism to one in which microvoid coalescence is more important.

For single-site failures ($\Delta\sigma < \sim 13$ MPa) particular flaws, typically 100 to 200 μm in size, could be located at the focus of some of the subsequent front loci; similar observations have been noted elsewhere under both laboratory [3, 11]and service [16] conditions. Referring again to Fig. 2, we emphasize that as cylic stress amplitude is reduced the failure process becomes more precisely localized at such severe, and presumably sparse, sites. Progress of the crack is initially brittle in character, only later involving voiding or plastic deformation. It is to be noted that service conditions involve precisely these low stress amplitudes, and thus that service failures are therefore likely to involve the growth of a single sharp crack, of fairly well-defined geometry throughout its life. These are the conditions of applicability of linear elastic fracture mechanics (LEFM), to which we now turn for a more detailed analysis.

3.2. LEFM analysis of fatigue crack growth

Application of LEFM theory involves the synthesis of two practical procedures. The first is an experimental evaluation of material properties as functions of the crack tip stress intensity factor, K; the second is evaluation (analytical or experimental) of K as a function of load and geometry in a particular service situation. In the problem of concern here the relevant material property is the cyclic rate of fatigue crack extension, da/dN, which can often be expressed as a power of the cyclic range, $\Delta K = K_{max} - K_{min}$, of K:

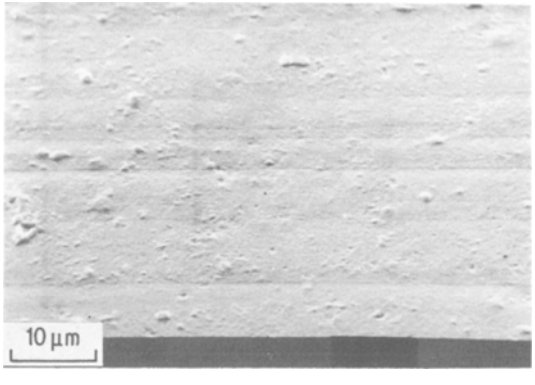

Figure 6 Detail of darker surface area in Fig. 4.

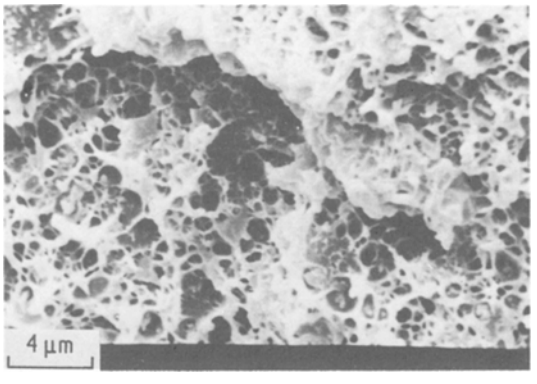

Figure 8 Further magnification of Fig. 7, showing extensive voiding.

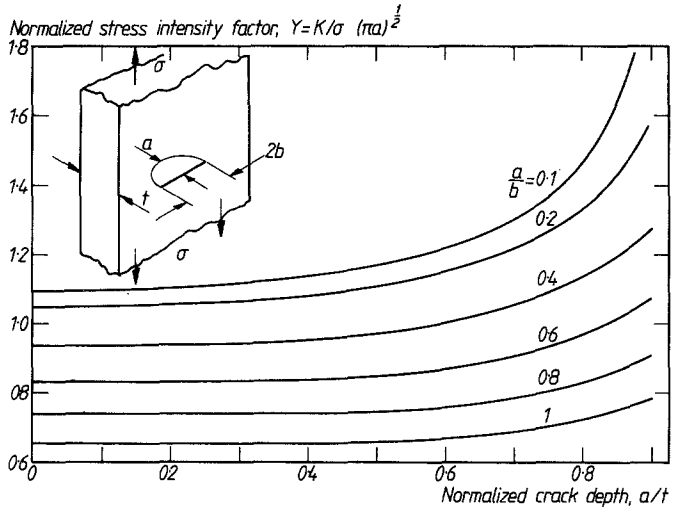

Figure 9 Stress intensity factor for a remotely stressed semi-elliptical surface crack (from Rooke and Cartwright [20]).

$$\frac{da}{dN} = C(\Delta K)^n, \qquad (2)$$

C and n being constants at specific conditions of such secondary variables as temperature, frequency, etc, here essentially fixed. This expression has been found to apply remarkably well to uPVC in tests at 20° C on rectangular flat plates with central through cracks parallel to the loaded edges [17–19]. Data from laminate, extruded sheet and pipe grades tested in the range $0.25 < \Delta K < 10\ \mathrm{MPa\,m^{1/2}}$ (four decades of crack growth rate) are all well characterized by $C = 10^{-7 \pm 0.25}$ (for da/dN in $\mathrm{m\,cycle^{-1}}$ and ΔK in $\mathrm{MPa\,m^{1/2}}$) and $n = 2.75$.

It must be pointed out, however, that for stress amplitudes below 20 MPa most cracks in pipe tests grew along pipe die spider weld lines, and that no data specifically derived from such material seem to be available.

The second prerequisite for LEFM analysis, the K solution for an internally cracked pipe, is readily available, particularly since thin-walled Class D and E pipes ($t < 0.1D$) have negligible through-thickness stress variation. Observations of the fracture surface have shown that, for a considerable proportion of its life, each crack had a semicircular plan shape, centred at a point on the bore. The solution for K at the deepest point of such a crack can be written as:

$$K = F_e\left(\frac{a}{b}, \frac{a}{t}\right)\sigma_e(\pi a)^{1/2}, \qquad (3)$$

a and b being crack depth and width, and F_e varying as in Fig. 9 (data from [20]). The effective stress, σ_e, is here the sum of a circumferential term given by Equation 1, and a crack face direct pressure addition. Since uniform pressure acting on all boundary surfaces will not open the crack, and therefore not affect K, it can be shown by superposition that the K solution for crack face pressure only is given by Equation 3 with $\sigma_e = p$, and the total K value by:

$$K = F_e\left(\frac{a}{b}, \frac{a}{t}\right)\left(1 + \frac{p}{\sigma}\right)\sigma(\pi a)^{1/2}. \qquad (4)$$

To the accuracy required here, the second term is 1.13 for Class D and 1.16 for Class E; this distinction is insignificant in practice and subsequent calculations are for the former.

Fig. 9 shows that F_e for a semicircular ($a = b$) crack remains virtually constant at 0.65 until its depth exceeds $a = 0.5t$. Crack front marks on the fracture surface showed that further extension was biased towards the axial direction, resulting in elliptical elongation with a/b falling. This compounds the increase in F_e due to the onset of finite thickness effects. thus K, additionally multiplied by $a^{1/2}$, will clearly "take off" at $a > 0.5t$. Because the fatigue crack growth rate rises exponentially as $\Delta K^{2.75}$, it can safely be assumed that relatively little of the total crack growth history was occupied by the second half of its extension. It will be demonstrated below that this is the case even if the increase in F_e is not taken into account.

These assumptions allow us to predict the fatigue lifetime, in cycles, of a pipe under a given circumferential stress range. From Equations 2 and 4 we have:

TABLE I Values of $(a_0^{-0.37} - a_f^{-0.37})$

Final crack length, a_f (μm)	Initial crack length, a_0 (μm)			
	50	100	200	400
2	30.73	21.34	14.10	8.11
3	32.18	22.79	15.55	9.50

$$\frac{da}{dN} = C(1.13\,F_e)^n(\Delta\sigma)^n(\pi a)^{n/2}, \quad (5)$$

which integrates to:

$$N = \left(\frac{1}{[1-n/2]\,C(1.13F_e)^n\,\pi^{n/2}\,(\Delta\sigma)^n}\right) \times (a_f^{1-n/2} - a_0^{1-n/2}) \quad (6)$$

a_0 and a_f being the initial and final crack depths. Substituting for constants yields:

$$N = (1.29 \times 10^7)\,(\Delta\sigma)^{-2.75}\,(a_o^{-0.37} - a_j^{-0.37}), \quad (7)$$

with $\Delta\sigma$ in MPa and a in m. Table I, showing values of the bracketted crack-length term, shows that considering 2 or 3 mm as the final crack length, has little significant effect on the predicted life of initially small cracks. The real effect, as discussed above, will be still less.

Fig. 10 shows the results of predicting fatigue lifetime from Equation 7 with $a_0 = 100$ and 200 μm. The agreement with the pipe lifetime data is encouraging, but not conclusive. The order of magnitude of a_0 lies between the molecular and the macroscopic, and might therefore relate to the impurities or inhomogeneities observed on this scale by microscopic examination of crack origins. The nature of this relationship is uncertain, and, considering the lack of systematic data on initial flaw sizes, it is best to regard a_0 as a measure of the severity of a defect (e.g. a weld line) equivalent to a crack depth. There is a tendency for the prediction to overestimate fatigue life at high stress levels, and underestimate at low ones. For high stresses, this is readily explained by the intervention, at some stage during crack extension, of additional ductile rupture processes, locally intensified by the presence of the crack as a stress raiser. This tends to blunt the crack, reduce the net section and, as already discussed, precipitates a switch-over to time-dependent stress rupture. For low stresses, the disparity is probably induced by limits on the sharp-crack, continuum mechanics basis of LEFM theory; this merits deeper discussion.

It has been shown that low stess levels reduce the number of flaws which subsequently develop into cracks, and it seems sensible to assume that only the largest will do so. However, this assumes that such flaws are sharp and crack-like from the outset, and this may not be so. A large, blunt flaw may be less deleterious under fatigue than a small, sharp one, and fractography may not necessarily distinguish a large "initial" flaw which has subsequently sharpened from one which has grown, during a initiation period, from a smaller, sharper crack. This competition between initiation and propagation mechanisms sets a minimum dimensional limit on LEFM validity. A second limit is imposed by the lower bound of observed crack growth rates. The integration of Equation 5 presupposed n to be constant down to ΔK levels at the initial flaw; while this may be so, existing data [17–19] do not extend far enough to serve as

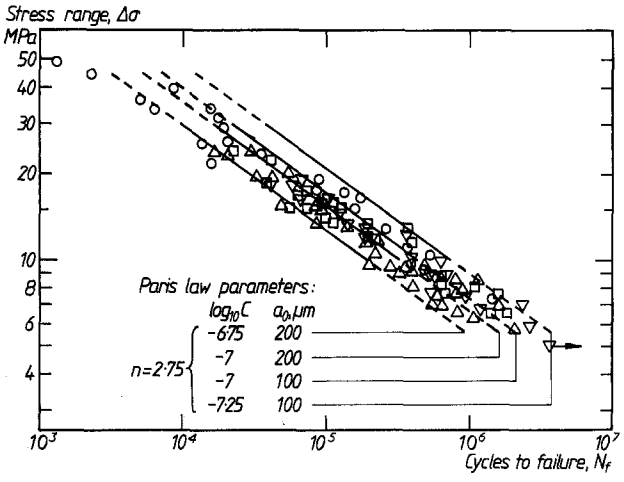

Figure 10 Comparison of data of Fig. 1, with prediction from LEFM.

evidence. The minimum ΔK levels used on this calculation prove to be extremely low (~ 0.07 MPa $m^{1/2}$) and would be associated with crack growth rates so low as to make data almost unobtainable at low frequencies, even if the extrapolation is valid. A further possibility is that a threshold – a vertical cut-off on the da/dN against ΔK characteristic – may intervene. It is most plausible, then, that LEFM consideration will govern pipe lifetimes for stress amplitudes in the 10 to 30 MPa range, as marked in Fig. 2.

3.3. LEFM approach to fracture surface morphology

The possibility has been raised of there being a change in the FCG mechanism in uPVC at very low cyclic growth rates. The fracture surface, consisting of material produced by the separation process, would be expected to indicate such a change, which should, moreover, be associated with a particular value of K (or ΔK). This section examines the relationship between the observed onset of a stress-whitened, microvoided surface texture, and the prevailing value of ΔK.

At the very lowest stress amplitudes investigated, this increase in reflectivity was gradual, but higher stresses caused an abrupt transition, leaving a well-defined semi-elliptical dark area (Fig. 4). SEM study revealed this to be increasingly voided at increasing crack depths, the actual transiton to a macroscopically whitened surface being due rather to the onset of larger-scale surface roughness and non-planar crack growth. However, more gradual surface transitions seemed to involve the simultaneous intensification of voiding and surface roughness. In this case rough and smooth regions seemed to coexist along the same crack front, and thus, under similar stress intensity factors. This situation is perhaps made possible by spatial variations in material properties.

The depth, a, at the midpoint of this gradual transition was measured for a number of specimens, using a travelling microscope. Fig. 11 shows $(\Delta\sigma)^2$ as a function of $1/a$, the slope m of which is related, using Equation 4 and Fig. 9, to ΔK at the surface transition:

$$\Delta K = 1.13 \times 0.65(\pi m)^{1/2}. \quad (8)$$

The value calculated, 0.27 MPa $m^{1/2}$, corresponds closely to the minimum level for which FCG rate data had been collected. A surface texture change at this level seems to warn of a change in FCG

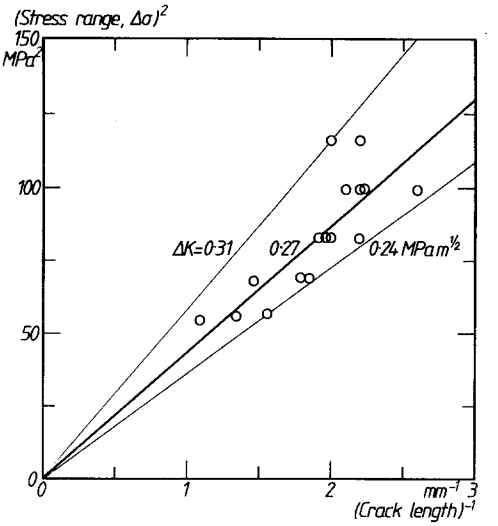

Figure 11 Stress-range size relationship for surface transitions as seen in Fig. 4, yielding corresponding stress intensity factor.

mechanism, and extrapolation of the material property data becomes precarious. Calculations show that at $\Delta\sigma = 12$ MPa, $\Delta K < 0.24$ MPa $m^{1/2}$ for only 34% of the pipe lifetime, whereas at $\Delta\sigma =$ 6 MPa this rises to 77%; thus for realsitic service stress levels, the "smooth-surface" FCG mechanism may operate for the majority of pipe lifetime.

3.4. LEFM analysis of crack front shape

The shape of abrupt surface texture transitions, crack front arrest markings due to machine shut-down, and the shapes of exposed part-through cracks, can all be used to monitor the plan geometry of a developing fatigue crack. Data from a number of specimens, expressed as the ellipse shape factor (a/b) as a function of normalized crack depth, is plotted in Fig. 12. Although correlation is not strong, it is conspicuous that shallow cracks tend to be roughly semicircular, but, as growth proceeds, they become relativley more extended along the axis. At the point of break-through at the outer surface, $a/b = 0.7$ to 0.8.

Let us examine the crack front shape in terms of any variation in K along it as it propagates. Some information on such circumferential variation is available [20] for the case of a part-circular surface crack of radius R in a semi-finite plate under uniform tensile stress. For a semicircular crack $(a = R)$, K varies smoothly between limits of K_d at the deepest point and, at the surface, $K_s \simeq 1.2K_d$. Since the crack growth

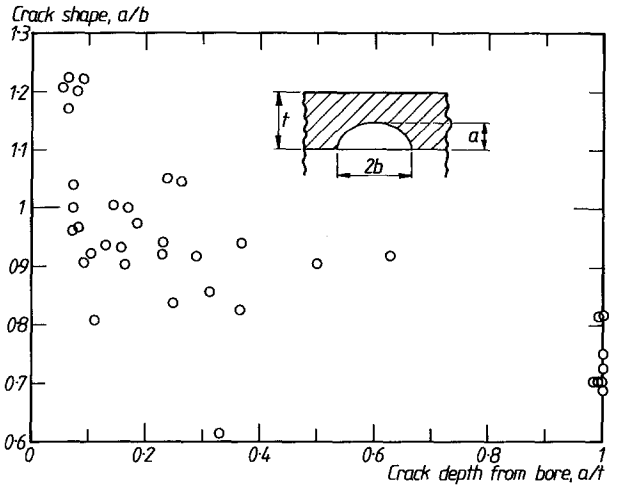

Figure 12 Crack shape as a function of penetration depth through pipe wall.

rate increases with ΔK, a mechanism exists to correct this by preferential axial extension until, at a ratio of $a \simeq 0.7R$, an approximately uniform K is achieved. The corresponding ellipse aspect ratio is $a = 0.73b$, and the assumption that such a plan shape achieves a uniform K distribution is qualitatively supported by data presented (though only for two a/b ratios) elsewhere [21].

Three factors which may help to account for the persistence of a semicircular crack front, along which K must vary, deserve consideration.

1. The influence of ΔK on crack growth rate, as expressed by n in Equation 2, may vary as the crack extends. This is unlikely, since an *increase* would be required, rather than the *decrease* associated with a fixed-ΔK threshold.

2. As considered above, LEFM theory may not apply rigorously to small cracks under these conditions (i.e. at extremely low ΔK). Other possible mechanisms for expansion of a planar damage zone – only later to become a crack – can be suggested, i.e. preferential diffusion of water-borne embrittling agents along the weld lines, or extension of a voided craze under the pressure of water trapped during pipe depressurization. Either of these alternatives could be investigated further, initially by using alternative pressurizing fluids.

3. A recent alternative approach to crack shape prediction in the double torsion fracture specimen [22, 23] has shown that K variation along a crack front is not prohibited by stability requirements; the understanding of three-dimensional crack shapes demands considerations beyond those discussed here.

4. Conclusions

1. No direct evidence has been found of a limiting stress amplitude below which fatigue failures do not occur.

2. Fatigue cracks at service stress amplitude levels are concentrated in the weld lines produced by the pipe die spider.

3. In this application, fracture mechanics theory provides a powerful analytical tool, and exposes the factors other than FCG which contribute to determining pipe lifetime. For circumferential stress amplitudes from 10 to 30 MPa a substantial part of the lifetime is taken up by FCG, at rates in agreement with those determined elsewhere. Above these stress levels gross plasticity and creep rupture occur; below them, we find that as yet undetermined mechanisms for initiation and growth of small cracks predominate.

4. These mechanisms, which generate smooth, featureless crack surfaces, occur at stress intensity factors below 0.27 MPa $m^{1/2}$, and are crucial to the performance of uPVC pipes under service conditions. Thus future fatigue investigations should be directed at this area.

Acknowledgements

This work was supported financially by the Polymer Engineering Directorate of the Science and Engineering Research Council and by the British Plastics Federation. The authors would also like to thank Professor J. G. Williams and Mr J. E. Miller for their contributions to the work.

References

1. R. W. HERTZBERG and J. A. MANSON, "Fatigue of Engineering Plastics" (Academic Press, New York, 1980).

2. G. P. MARSHALL and M. W. BIRCH, *Plastics and Rubber Processing and Applications* **2** (1982) 369.
3. D. R. MOORE, K. V. GOTHAM and M. J. LITTLEWOOD, Proceedings of the 4th International Conference on Plastic Pipes, Brighton, 1979 (PRI, London, 1979) paper 27.
4. K. V. GOTHAM and M. J. HITCH, *Pipes and Pipelines Int.* **20** (1975) 10.
5. *Idem, Brit. Polym. J.* **10** (1978) 47.
6. A. GONZE and C. RODEYNS, *Publ. Inst. Kunst Univ Stuttgart* **10** (1972) 478.
7. H. W. VINSON, Proceedings of the International Conference on Underground Plastic Pipe, New Orleans, 1981 (ASCE, 1981) p. 485.
8. H. DATENE, L. E. JANSON and P. VALIMAA, *Kunststoffe* **67** (1977) 466.
9. M. A. CHRISTIE and B. PHELPS, International Conference on Fatigue in Polymers, London, 1983 (PRI, London, 1983) paper 17.
10. C. E. KIRSTEIN, *Publ. Inst. Kunst Univ. Stuttgart* **10** (1972) 1.
11. S. H. JOSEPH, Proceedings of the 4th International Conference on Plastic Pipes, Brighton, 1979 (PRI, London 1979) paper 28.
12. R. T. HUCKS, *J. AWWA* July (1972) 443.
13. R. CROMBRUGGE, R.I.L.E.M. Symposium, Liege, 1974 (University of Liege, 1974) p. 448.
14. I. ONISHI, H. KIMOZA and M. UEMATU, *J. Jap. Weld Soc.* **35** (1966) 50.
15. ICI, "Designing with unplasticised polyvinyl chloride" (ICI, Welwyn Garden City) Technical Service Note W121.
16. P. C. KIRBY, Proceedings of the International Conference on Underground Plastic Pipe, New Orleans, 1981 (ASCE, 1981) p. 254.
17. P. S. LEEVERS, L. E. CULVER and J. C. RADON, *Eng. Fract. Mech.* **11** (1979) 487.
18. P. S. LEEVERS, PhD thesis, University of London (1979).
19. A. M. B. A. OSORIO and J. G. WILLIAMS, International Conference on Fatigue in Polymers, London, 1983 (PRI, London, 1983) paper 7.
20. D. P. ROOKE and D. J. CARTWRIGHT, "Compendium of Stress Intensity Factors" (HMSO, London, 1976).
21. F. W. SMITH and D. R. SORENSEN, *Int. J. Fract.* **12** (1976) 47.
22. B. STALDER and H. H. KAUSCH *J. Mater. Sci.* **17** (1982) 2481.
23. P. S. LEEVERS, *ibid* **17** (1982) 2469.

Received 19 January
and accepted 13 March 1984